Journal of Peptide Science
*J. Pept. Sci.* 2008; **14**: 429–435
Published online 6 November 2007 in Wiley InterScience (www.interscience.wiley.com). DOI: 10.1002/psc.934

JOURNAL OF PEPTIDE SCIENCE

# A minor $\beta$-structured conformation is the active state of a fusion peptide of vesicular stomatitis virus glycoprotein‡

**CAROLINA G. SARZEDAS,[a,b]§ CARLA S. LIMA,[a]§ MARIA A. JULIANO,[c] LUIZ JULIANO,[c] ANA PAULA VALENTE,[a,b] ANDREA T. DA POIAN[a]* and FABIO C. L. ALMEIDA[a,b]**

[a] Instituto de Bioquímica Médica, Programa de Biologia Estrutural, Universidade Federal do Rio de Janeiro, Rio de Janeiro, RJ 21941-590, Brazil
[b] Centro Nacional de Ressonância Magnética Nuclear Jiri Jonas (CNRMN), Universidade Federal do Rio de Janeiro, Rio de Janeiro, RJ 21941-590, Brazil
[c] Departamento de Biofísica, Escola Paulista de Medicina, UNIFESP, Rua Três de Maio, 100, São Paulo 04044-020, Brazil

*Received 27 June 2007; Revised 20 July 2007; Accepted 14 August 2007*

**Abstract:** Entry of enveloped animal viruses into their host cells always depends on a step of membrane fusion triggered by conformational changes in viral envelope glycoproteins. Vesicular stomatitis virus (VSV) infection is mediated by virus spike glycoprotein G, which induces membrane fusion at the acidic environment of the endosomal compartment. In a previous work, we identified a specific sequence in the VSV G protein, comprising the residues 145–164, directly involved in membrane interaction and fusion. In the present work we studied the interaction of pep[145–164] with membranes using NMR to solve the structure of the peptide in two membrane-mimetic systems: SDS micelles and liposomes composed of phosphatidylcholine and phosphatidylserine (PC : PS vesicles). The presence of medium-range NOEs showed that the peptide has a tendency to form *N*- and *C*-terminal helical segments in the presence of SDS micelles. Analysis of the chemical shift index indicated helix–coil equilibrium for the *C*-terminal helix under all conditions studied. At pH 7.0, the *N*-terminal helix also displayed a helix–coil equilibrium when pep[145-164] was free in solution or in the presence of PC : PS. Remarkably, at the fusogenic pH, the region of the *N*-terminal helix in the presence of SDS or PC : PS presented a third conformational species that was in equilibrium with the helix and random coil. The *N*-terminal helix content decreases pH and the minor $\beta$-structured conformation becomes more prevalent at the fusogenic pH. These data point to a $\beta$-conformation as the fusogenic active structure-which is in agreement with the X-ray structure, which shows a $\beta$-hairpin for the region corresponding to pep[145-164]. Copyright © 2007 European Peptide Society and John Wiley & Sons, Ltd.

*Supplementary electronic material for this paper is available in Wiley InterScience at http://www.interscience.wiley.com/jpages/1075-2617/suppmat/*

**Keywords:** membrane fusion; vesicular stomatitis virus; NMR; structure

## INTRODUCTION

Virus infection depends on the delivery of viral genome and accessory proteins into the cytosol or, in some cases, into the nucleus of the host cell, thereby by-passing or modifying the barrier properties imposed by the plasma membrane. In the case of enveloped viruses, the entry process involves the fusion of their lipid envelope with the plasma or endosomal membranes of the host cell [1–4]. Membrane fusion induced by viruses is mediated by viral fusion glycoproteins, which acquire the fusogenic activity after conformational changes triggered either by their interaction with a specific virus receptor on the cell surface or by the acidic pH of the endosomal medium [5,6]. It is believed that these conformational changes lead to the exposure of a short sequence in the glycoprotein, which is directly involved in the interaction with the target membrane during the fusion reaction, known as the *fusion peptide* [7].

Vesicular stomatitis virus (VSV) belongs to the Rhabdoviridae family, a group of enveloped, negative, single-strand RNA viruses. The VSV envelope contains many copies of a single transmembrane glycoprotein, the G protein that forms trimeric spikes on the virus surface. VSV G protein is involved in virus attachment to the host cell surface, and in the membrane fusion mediated by the virus that occurs at the endosomal compartment where the acidic pH induces conformational changes on G protein [8,9].

In previous works, we have demonstrated that a synthetic peptide corresponding to amino acids 145–164 of G protein (pep[145–164]), which is the VSV binding site to phosphatidylserine (PS) [10], was as efficient as the whole virus in catalyzing fusion at pH 6.0 [11,12]. Several pieces of evidence in the literature suggest a direct role for PS in VSV entry

* Correspondence to: Andrea T. Da Poian, Instituto de Bioquímica Médica, Universidade Federal do Rio de Janeiro, Rio de Janeiro, RJ 21941-590, Brazil; e-mail: dapoian@bioqmed.ufrj.br
‡ This article is part of the Special Issue of the Journal of Peptide Science entitled "2nd workshop on biophysics of membrane-active peptides".
§ The authors contributed equally to this work.

into the host cell [13–15]. This phospholipid has also shown to be essential for VSV–membrane interactions at neutral and fusogenic pHs [16,17]. The identification of PS binding segments in several rhabdovirus G proteins [10] and the fact that antibodies against this segment of the G protein of a salmonid rhabdovirus were able to inhibit both PS binding to this virus and virus-induced cell to cell fusion [18] suggest a direct participation of the PS binding site in rhabdovirus entry.

Whether pep[145–164] has a direct participation in VSV fusion or this segment only takes part of the membrane-interacting regions of the G protein is still an open question. Much data from other groups and us [10–18] strongly indicate a direct interaction between pep[145–164] and the target membrane. As already shown for the whole virus, peptide–membrane interaction is specific to PS [17] and dependent on the presence of His in its sequence, whose substitution by Ala or modification with diethylpyrocarbonate (DEPC) inhibits peptide fusogenic properties. This is in agreement with our previous data showing that the G protein His-modified with DEPC avoids the virus entry into the host cell both *in vitro* and *in vivo* [19].

The main goal of the present work was the understanding of the structural requirements for the pep[145–164] to induce fusion. We used NMR to solve the structure of the peptide in SDS micelles and liposomes composed of phosphatidylcholine and phosphatidylserine (PC : PS vesicles). We showed that the peptide forms two helical segments in the presence of SDS micelles. Analysis of chemical shift index indicated that the *N*-terminal helix is in equilibrium with other minor conformational states, and that the *N*-terminal helix content decreases at the fusogenic pH. The analysis of pep[145–164] bound to PC : PS vesicles also showed the presence of the *N*-terminal helix at pH 7.0, but revealed that a minor extended conformation becomes more prevalent at the fusogenic pH. These data point to a $\beta$-conformation as the fusogenic active structure – which is in agreement with the X-ray structure – which shows a $\beta$-hairpin for region corresponding to pep[145–164] [20].

## MATERIAL AND METHODS

### Peptide Synthesis

The VSV G protein peptide corresponding to the sequence between amino acids 145 and 164 (VTPHHVLVDEYTGEWVD SQF-$NH_2$) was synthesized by solid phase using the Fmoc methodology. All protected amino acids were purchased from Calbiochem-Novabiochem (San Diego, USA) or from Neosystem (Strasbourg, France). The syntheses were carried out in an automated bench-top, simultaneous multiple solid-phase peptide synthesizer (PSSM 8 system from Shimadzu). The final deprotected peptides were purified by semipreparative HPLC using an Econosil C-18 column (10 μm, 22.5 × 250 mm) and a two-solvent system: (A) trifluoroacetic acid/$H_2O$ (1 : 1000, v/v) and (B) trifluoroacetic acid/acetonitrile/$H_2O$ (1 : 900 : 100, v/v/v). The column was eluted at a flow rate of 5 ml $min^{-1}$ with a 10, 30–50 or 60% gradient of solvent B over 30 or 45 min. Analytical HPLC was performed using a binary HPLC system from Shimadzu with an SPD-10AV Shimadzu UV/vis detector coupled to an Ultrasphere C-18 column (5 μm, 4.6 × 150 mm), which was eluted with solvent systems A1 ($H_3PO_4/H_2O$, 1 : 1000, v/v) and B1 (acetonitrile/$H_2O$/$H_3PO_4$, 900 : 100 : 1, v/v/v) at a flow rate of 1.7 ml $min^{-1}$ and a 10–80% gradient of B1 over 15 min. The eluted materials from the HPLC column were monitored by their absorbance at 220 nm. The molecular mass and purity of synthesized peptides were checked by MALDI-TOF mass spectrometry (TofSpec-E, Micromass) and/or peptide sequencing using a protein sequencer PPSQ-23 (Shimadzu Tokyo, Japan).

### Preparation of Liposomes

The phosphatidylcoline (PC) from chicken egg and phosphadylserine from bovine brain were purchased from Avanti Polar Lipid. Phospholipds in a molar ration of 3 : 1 (PC : PS) were dissolved in chloroform and evaporated under nitrogen. The lipid film was resuspended in 20 mM phosphate buffer (pH 7.0 or 6.0) and 50 mM NaCl in a final total lipid concentration of 20 mM (15 mM of PC plus 5 mM of PS). The vesicles were extruded through a membrane (0.22 μm) during 10 cycles, forming unilamellar vesicles.

### NMR Sample Preparation

For experiments using the peptide free in solution, the lyophilized peptide sample was solubilized in 20 mM phosphate buffer (pH 6.0 or 7.5) and 50 mM NaCl to a final concentration of 1 mM. For experiments with SDS micelles, perdeutered SDS in a final concentration of 400 mM was added to the 1 mM peptide solution in 20 mM phosphate buffer (pH 6.0 or 7.5) and 50 mM NaCl. Perdeuterated SDS was purchased from Cambridge Isotopes Inc., Boston (USA). The sample for experiments with vesicles was prepared with the peptide at 1 mM final concentration in the presence of PC : PS vesicles (3 : 1) in 20 mM phosphate buffer and 50 mM NaCl.

### NMR Experiments

The NMR experiments were acquired in a Bruker spectrometer DRX-600 MHz and at 25 °C. All NOESY and TOCSY spectra were acquired using 4096 × 512 complex points, digital quadrature detection mode and States-TPPI for the frequency discrimination in the indirect dimension.

Before carrying out the experiments in SDS micelles, a series of one-dimensional $^1H$ spectra of pep[145–164] were acquired with increasing SDS concentration (40 to 400 mM, data not shown). The lines became sharper, reaching a limit after 200 mM of SDS. The increase in SDS concentration results in a shift towards the bound state, leading to a decrease in conformational exchange and a sharpening of resonances. Thus, all experiments were carried out at 400 mM SDS with the peptide in the SDS-bound state. For the NOESY spectra in SDS micelles, we used a mixing time of 120 ms. This value was chosen on the basis of an NOE build-up curve. For the



DOI: 10.1002/psc

transfer NOESY spectra in the presence of vesicles, three different mixing times (60, 120 and 160 ms) were used. The spectrum that was used for most of the analyses was NOESY with a mixing time of 120 ms. For each of the transfer NOESY experiments in the presence of vesicles, we ran an identical experiment under the same condition, but without the vesicles. The spectra were processed using NMR Pipe [21] and analyzed using NMR View v5.02 [22].

## RESULTS

### Peptide Interaction with SDS Micelles

Two-dimensional NOESY and TOCSY experiments of pep[145–164] were performed in the presence of SDS micelles at pH 6.0 and compared with data obtained at pH 7.5. Full assignment of the peptide was obtained using the sequential methodology proposed by Wüthrich (1986) [23]. Figure 1(A) shows a summary of the NOEs assigned at pH 6.0 and 7.5. Consecutive, medium-range NOEs $\alpha$N ($i$, $i+3$), $\alpha$N ($i$, $i+4$), $\alpha\beta$ ($i$, $i+3$) were observed, typical of helical structures. In SDS, pep[145–164] has a tendency to form two helical spans. The *N*-terminal helix was observed from residues T146 to L151 at pH 7.5 and from H149 to Y155 at pH 6.0. The *C*-terminal helix was observed from residues V160 to F165 at pH 7.5 and from W159 to Q164 at pH 6.0.

Helical structural tendency is always followed by upfield chemical shift deviation for the hydrogen linked to the $\alpha$-carbon ($\alpha$H) [24]. Figure 1(B) shows that this was the case with the *C*-terminal helix at both pHs. On the other hand, the *N*-terminal helix displayed NOEs typical of helix but chemical-shift index typical of random-coil or extended structures. The fact that the typical NOEs of helix were not followed by negative H$\alpha$ chemical-shift deviations could be explained by the presence of minor conformation(s) contributing positively to the chemical-shift values. Positive chemical shift indexes are typical of extended conformation or $\beta$-structures [24], suggesting that the *N*-terminal helix is in fast equilibrium with these structural species.

The pH-driven transition toward the fusogenic conformation was evaluated by the number and the intensities of the NOEs in the two pHs. The number of NOEs typical of the helix was higher at pH 7.5 than at the fusogenic pH (6.0) (Figure 1(A)). In accordance with the number of NOEs, the changes in the normalized intensities increase for the $\beta$-related NOEs ($\alpha$N ($i$, $i+1$)) and decrease for the helix-related NOEs ($\alpha$N ($i$, $i+3$) and ($\alpha\beta$ ($i$, $i+3$)) (Figure 1(C)). These data suggest that the content of helix decreases in the fusogenic state.

### Peptide Interaction with PC : PS Vesicles

As shown in the previous section, pep[145–164] has the tendency to form two helical segments in SDS. In the *N*-terminal end there is equilibrium between the helical conformation and other structures, which could be extended or random coil. In addition, the helix content decreases at the fusogenic pH. These observations raised the question whether the fusogenic conformation is the prevalent helical conformer or the $\beta$-structured conformer. To answer this question we performed transfer NOESY experiments in the presence of PC : PS vesicles at neutral and fusogenic pHs, which mimic better the microenvironment experienced by viral glycoprotein during the infection of the host cell.

The NOESY spectra of pep[145–164] free in aqueous solution at both pH 6.0 and 7.0 showed a small number of NOEs, which corresponded exclusively to inter-residue NOEs (Figure 2(A), left panels). However, the NOESY spectra in presence of PC : PS vesicles at both pHs displayed a great increase in the number of NOEs, a result of the interaction of pep[145–164] with the membrane (Figure 2(A), right panels). These data also show that the interaction occurred in the fast/intermediate timescale, typically microseconds. The number and intensity of transfer NOEs were much higher at pH 6.0 than at pH 7.0. This evidences that the interaction at the fusogenic pH is stronger.

In the presence of vesicles, the number of transfer NOEs was not enough for structural calculation. However, the analysis of the H$\alpha$ chemical-shift perturbations induced by the interaction gave important structural insights of the peptide in the membrane-bound state. Figure 2(B) shows the chemical-shift difference between the H$\alpha$ of pep[145–164] in the presence of PC : PS vesicles and the expected values for a random coil. Negative values for the *C*-terminal helix region were observed, indicating the presence of helix–coil equilibrium at this segment of the peptide at both pHs. The *N*-terminal helix also displayed negative values at pH 7.0 for the segment V152–Y155, typical of helix–coil equilibrium. The profile obtained for pep[145–164] in PC : PS at pH 7.0, presented in Figure 2(B), was very similar to that obtained for free pep[145–164] in aqueous solution at both pH 6.0 and 7.0 (Supplementary Figure 1), meaning that when pep[145–164] is free in solution there is also helix–coil transition in the region of both *N*-terminal (segment V152–Y155) and *C*-terminal helices (segment W159–Q163). Remarkably, the region of the *N*-terminal helix displayed a more complex behavior at the fusogenic pH. The values of H$\alpha$ chemical-shift deviation became less negative, or even positive, for some residues of the segment V152–Y155. This indicates that there is another conformational species in equilibrium with the helix and coil structures which produces positive H$\alpha$ deviations, suggesting that the fusogenic conformation is an extended conformation or a $\beta$-structure.



DOI: 10.1002/psc

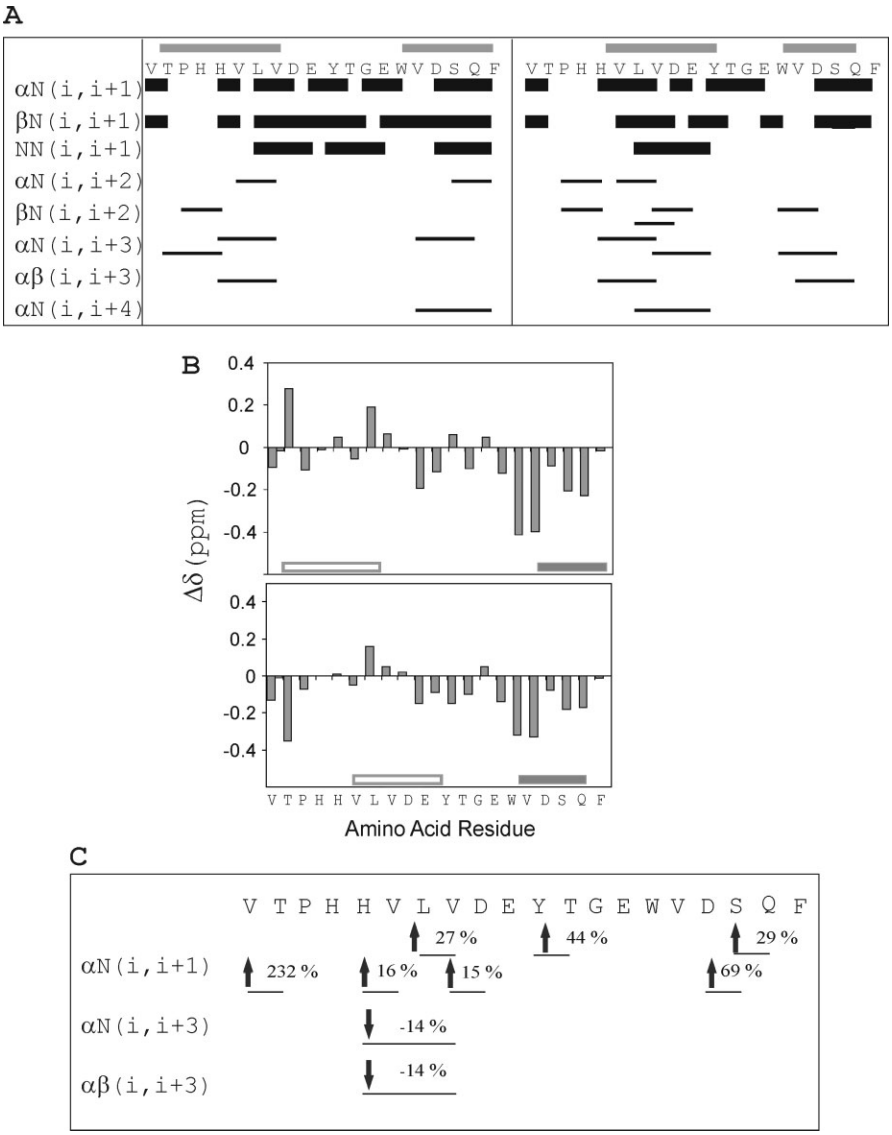


**Figure 1** (A) NOE summary of the pep[145–164] in SDS micelles, showing the sequential and medium-range NOEs. On the left are the results at pH 6.0, and on the right, at pH 7.5. The bars at the top represent the helical regions predicted from the presence of ($i$, $i+3$) and ($i$, $i+4$) NOEs. (B) Difference of H$\alpha$ chemical shift for each residue of pep[145–164] in SDS micelles and the expected random-coil values ($\Delta\delta$) as a function of the residue name. At the top are the results at pH 6.0, and at the bottom, at pH 7.5. The solid bars indicate the helical regions predicted by the NOEs and confirmed by chemical-shift deviations. The hollow bars indicate the helical regions predicted by the NOEs but not confirmed from chemical-shift deviation. (C) NOE summary of the pep[145–164] in SDS micelles showing only the cross-peaks that are common for both pH 6.0 and 7.5. For each NOE we show the comparison of the normalized intensities at pH 6.0 and 7.5. The normalization was obtained by dividing the intensity of the cross-peaks with the intensity of the corresponding diagonal peak. The arrows indicate whether the normalized intensity increases (pointing up) or decreases (point down) on going from pH 7.5 to 6.0. We have not considered the effect of overlaps in the diagonal peaks in the NOE normalization because they are present both at pH 6.0 and 7.5. All experiments were carried out at 20 mM phosphate buffer, 50 mM NaCl and 400 mM SDS.

## DISCUSSION

In the present work we studied the interaction of pep[145–164] with two different membrane mimetic systems: SDS micelles and PC : PS vesicles. The study in SDS micelles enabled higher-resolution structural information of the peptide in the membrane-bound conformation. PC : PS vesicles better mimic the microenvironment experienced by viral glycoprotein during the infection of the host cell. Moreover, NMR data of pep[145–164] in PC : PS yielded qualitative structural features that are very informative for mapping the residues involved in the interaction with the membrane and also in the secondary structure changes.

The pep[145–164] showed a tendency, mapped by the presence of NOEs and H$\alpha$ chemical-shift deviation, to form helixes in two segments of the sequence, at



DOI: 10.1002/psc

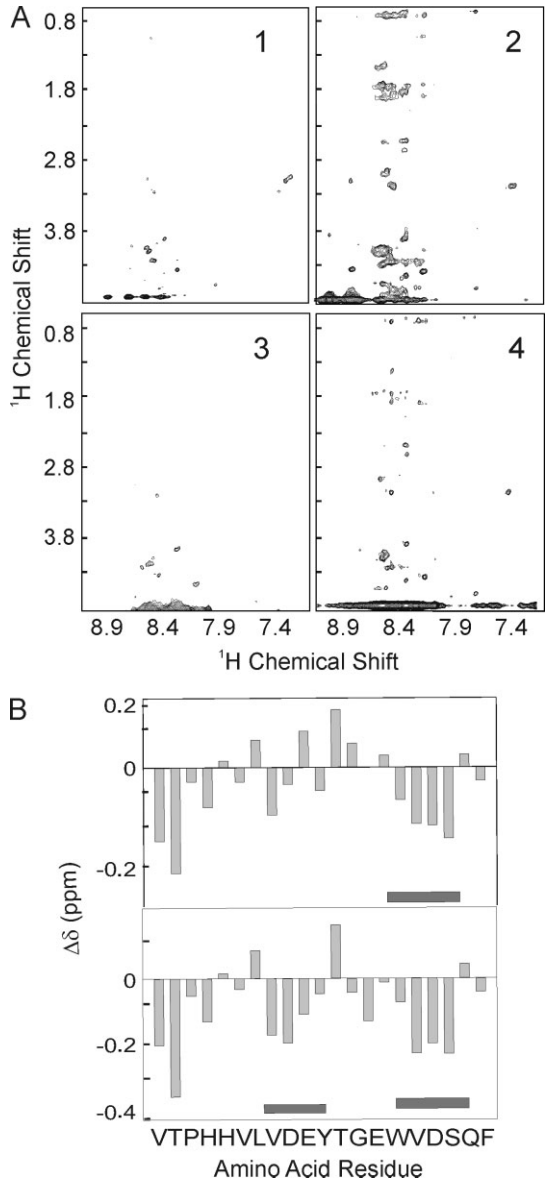


**Figure 2** (A) NOESY spectra of pep[145–164] in the presence (A2 and A4) and absence of PC : PS vesicles (A1 and A3). The spectra at pH 6.0 are at the top (A1 and A2) and at pH 7.0 are at the bottom (A3 and A4). (B) Difference of Hα chemical shift of pep[145–164] in the presence of PC : PS vesicles and the expected random-coil values (Δδ) as a function of the residue name. At the top are the results at pH 6.0 and at the bottom, at pH 7.5. The bars indicate the helical regions predicted from the Hα chemical-shift deviations. All experiments were carried out at 20 mM phosphate buffer, 50 mM NaCl and PC : PS, as described in 'Materials and Methods'.

the *N*- and *C*-termini. As depicted in Figure 3, the *C*-terminal helix displays helix–coil equilibrium in all the studied conditions, producing ($i$, $i+3$) medium-range NOEs and negative Hα chemical-shift deviations. The *N*-terminal helix, on the other hand, showed a more complex equilibrium that appears only at the fusogenic pH, both in the presence of SDS and in the presence of PC : PS vesicles.

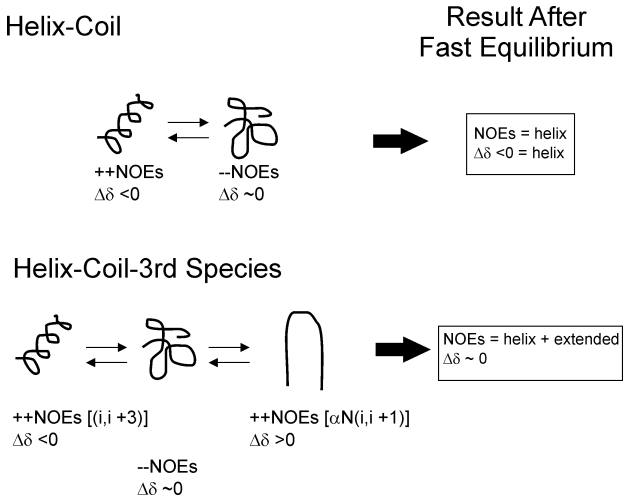


**Figure 3** Schematic representation of conformational equilibrium of pep[145–164]. At the top is represented the helix–coil equilibrium. The helical conformer results in ($i$, $i+3$) NOEs and negative Hα chemical-shift deviation ($\Delta\delta < 0$). The random-coil conformation results in absence of or weak NOEs and $\Delta\delta$ close to zero. The expected result of the two species in fast equilibrium would be the presence of NOEs typical of helix and $\Delta\delta < 0$. At the bottom is represented a more complex equilibrium among helix, coil and a third species. The helical conformer results in ($i$, $i+3$) NOEs and $\Delta\delta < 0$. The random-coil conformation results in the absence of or weak NOEs and $\Delta\delta$ close to zero. If the third species is an extended or β-structured conformer, strong αN ($i$, $i+1$) and $\Delta\delta > 0$ would be expected. The expected result of the three species in fast equilibrium would be the presence of NOEs typical of helix and typical of β-structure (αN ($i$, $i+1$)) and $\Delta\delta \sim 0$.

It has been extensively demonstrated that many helicoidal peptides undergo helix–coil equilibrium [25–27]. Since helix produces negative Hα chemical-shift deviations, and random coil results in values close to zero, helix–coil equilibrium will always bring in negative values of Hα chemical-shift deviations. The equilibrium of helix, random coil and a third conformational species that produces positive Hα chemical-shift deviations would result in values slightly positive or zero, as obtained for the equilibrium in which the *N*-terminal helix is involved. This third species is expected to be an extended conformation such as a β-structure (Figure 3(A)). The formation of the β-structure also explains the stronger αN ($i$, $i+1$) and weaker αN ($i$, $i+3$) NOEs.

The model shown in Figure 3 takes into consideration a new view of binding that, instead of presuming an induced fit of the peptide to the interface, assumes the existence of pre-existent, ordered conformational states in equilibrium (for a review see [Ref.28]). Here we mapped the existence of a third conformational state in extended conformation. This β-structured state represents a minor conformation when the peptide is free in solution. However, the presence of the membrane interface at the fusogenic



DOI: 10.1002/psc

conditions shifted the population toward this state, increasing its contribution to the observed chemical-shift deviation. Our previous calorimetric studies indicated that peptide binding to membranes depends on electrostatic interactions, suggesting that the binding might be mediated by a direct interaction between the negative charges of PS and the positively charged peptide His residues at the fusogenic pH [17]. These His residues are located in the *N*-terminal segment of the peptide, the region that forms the extended structure. Thus, their protonation (p*K*a $\sim$ 6.0) could be driving and stabilizing the peptide interaction with the membrane.

It is interesting to compare the findings of a minor $\beta$-structured conformation with the recently solved X-ray structures of the ectodomain of the VSV G-protein in the fusogenic [20] and pre-fusogenic state [29]. These data point to a $\beta$-conformation as the fusogenic active structure – in agreement with the X-ray structure – which shows not a helix but a $\beta$-hairpin for the region corresponding to pep[145–164]. The $\beta$-hairpin that could be the minor conformation for the pep[145–164] free in solution is the major conformation in the whole protein, possibly stabilized by tertiary contacts with the rest of the G protein. The solved X-ray structures revealed that pep[145–164] is not at the tip of the fusogenic domain [20,29], where the putative fusion peptide was supposed to be. However, much data, from other groups and us [10–18], strongly indicate a direct interaction between pep[145–164] and the target membrane. Probably, pep[145–164] might participate in VSV fusion as an accessory segment.

## CONCLUSIONS

One of the main achievements of the present work was to give structural insights on the membrane-active region of pep[145–164]. NMR studies indicated the presence of equilibrium among several conformational species in pep[145–164]. The helical species is prevalent in the presence of SDS micelles. We demonstrated the presence of a $\beta$-structured minor conformation within the *N*-terminal region of the peptide. The equilibrium shifts toward this $\beta$-structured conformation when the peptide is at the fusogenic pH, in the presence of membranes. The residues for which we observed the highest changes when the pH was shifted from 7.0 to 6.0 in the presence of PC : PS vesicles were Val152-Asp153-Glu154 and Tyr155. These residues take part of the $\beta$-hairpin in the X-ray structure of VSV G protein, which is formed by the residues Leu151-Val152-Asp153-Glu154 (first $\beta$-strands); Tyr155, Thr156 ($\beta$-turn); and Gly157-Glu158-Trp159-Val160 (second $\beta$-strand).

## Supplementary Material

Supplementary electronic material for this paper is available in Wiley InterScience at: http://www.interscience.wiley.com/jpages/1075-2617/suppmat/

## Acknowledgements

We acknowledge the funds from International Centre for Genetic Engineering and Biotecnology (ICGEB, Trieste, Italy), Conselho Nacional de Desenvolvimento Científico e Tecnológico (CNPq, Brazil), Fundação Carlos Chagas Filho de Amparo à Pesquisa do Estado do Rio de Janeiro (FAPERJ, Brazil), Millennium Institute of Structural Biology in Biotechnology and Biomedicine and Fundação de Amparo a Pesquisa do Estado de São Paulo (FAPESP).

## REFERENCES

1. Skehel J, Wiley DC. Receptor binding and membrane fusion in virus entry: The Influenza Hemagglutinin. *Annu. Rev. Biochem.* 2000; **69**: 531–569.
2. Eckert DM, Kim PS. Mechanisms of viral membrane fusion and its inhibition. *Annu. Rev. Biochem.* 2001; **70**: 770–810.
3. Harrison PM, Zheng D, Zhang Z, Carriero N, Gerstein M. Transcribed processed pseudogenes in the human genome: an intermediate form of expressed retro-sequence lacking protein-coding ability. *Nucleic Acids Res.* 2005; **33**: 2374–2383.
4. Da Poian AT, Carneiro FA, Stauffer F. Viral membrane fusion: is glycoprotein G of rhabdoviruses a representative of a new class of viral fusion proteins? *Braz. J. Med. Biol. Res.* 2005; **38**: 813–823.
5. Kielian M, Rey FA. Virus membrane-fusion proteins: more than one way to make a hairpin. *Nat. Rev. Microbiol.* 2006; **4**: 67–76.
6. Weissenhorn W, Hinz A, Gaudin Y. Virus membrane fusion. *FEBS Lett.* 2007; **581**: 2150–2155.
7. Epand RM. Fusion peptides and the mechanism of viral fusion. *Biochim. Biophys. Acta.* 2003; **1614**: 116–121.
8. Gaudin Y, Tuffereau C, Segretain D, Knossow M, Flamand A. Reversible conformational changes and fusion activity of rabies virus glycoprotein. *J. Virol.* 1991; **65**: 4853–4859.
9. Da Poian AT, Gomes AMO, Coelho-Sampaio T. Kinetics of intracellular viral disassembly and processing probed by Bodipy fluorescence dequenching. *J. Virol. Methods* 1998; **70**: 45–58.
10. Coll JM. Synthetic peptides from the heptad repeats of the glycoproteins of rabies, vesicular stomatitis and fish rhabdoviruses bind phosphatidylserine. *Arch. Virol.* 1997; **142**: 2089–2097.
11. Carneiro FA, Stauffer F, Lima CS, Juliano MA, Juliano L, Da Poian AT. Membrane fusion induced by vesicular stomatitis virus depends on histidine protonation. *J. Biol. Chem.* 2003; **278**: 13789–13794.
12. Carneiro FA, Vandenbussche G, Juliano MA, Juliano L, Ruysschaert JM, Da Poian AT. Charged residues are involved in membrane fusion mediated by a hydrophilic peptide located in vesicular stomatitis virus G protein. *Mol. Membr. Biol.* 2006; **23**: 396–406.
13. Schlegel R, Willingham MC, Pastan IH. Saturable binding sites for vesicular stomatitis virus on the surface of Vero cells. *J. Virol.* 1982; **43**(3): 871–875.
14. Schlegel R, Tralka TS, Willingham MC, Pastan I. Inhibition of VSV binding and infectivity by phosphatidylserine: is phosphatidylserine a VSV-binding site? *Cell* 1983; **32**(2): 639–646.
15. Mastromarino P, Conti C, Goldoni P, Hauttecoeur B, Orsi N. Characterization of membrane components of the erythrocyte involved in vesicular stomatitis virus attachment and fusion at acidic pH. *J. Gen. Virol.* 1987; **68**(Pt 9): 2359–2369.

16. Carneiro FA, Bianconi ML, Weissmüller G, Stauffer F, Da Poian AT. Membrane recognition by vesicular stomatitis virus involves enthalpy-driven protein-lipid interactions. *J. Virol.* 2002; **76**(8): 3756–3764.
17. Carneiro FA, Lapido-Loureiro PA, Cordo SM, Stauffer F, Weissmuller G, Bianconi ML, Juliano MA, Juliano L, Bisch PM, Da Poian AT. Probing the interaction between vesicular stomatitis virus and phosphatidylserine. *Eur. Biophys. J.* 2006; **35**: 145–154.
18. Estepa A, Coll JM. Pepscan mapping and fusion-related properties of the major phosphatidylserine-binding domain of the glycoprotein of viral hemorrhagic septicemia virus, a salmonid rhabdovirus. *Virology* 1996; **216**: 60–70.
19. Stauffer F, De Miranda J, Carneiro FA, Salgado LT, Machado G, Da Poian AT. Inactivation of vesicular stomatitis virus through inhibition of membrane fusion by chemical modification of the viral glycoprotein. *Antiviral Res.* 2007; **73**: 31–39.
20. Roche S, Bressanelli S, Rey FA, Gaudin Y. Crystal structure of the low-ph form of vesicular stomatitis virus glycoprotein G. *Science* 2006; **313**: 187–191.
21. Delaglio F, Grzesiek S, Zhu G, Vuister GM, Pfeifer J, Bax AJ. NMRPipe: A multidimensional spectral processing system based on UNIX pipes. *J. Biomol. NMR* 1995; **3**: 277–293.
22. Johnson BA, Blevins RA. NMR View: A computer program for the visualization and analysis of NMR data. *J. Biomol. NMR* 1994; **4**: 603–614.
23. Wüthrich K. *NMR of Proteins and Nucleic Acids*. John Wiley and Sons: New York, 1986.
24. Wishart DS, Sykes BD, Richards FM. Relationship between nuclear magnetic resonance chemical shift and protein secondary structure. *J. Mol. Biol.* 1991; **222**(2): 311–333.
25. Muñoz V, Serrano L. Elucidating the folding problem of helical peptide using empirical parameters. *Nat. Struct. Biol.* 1994; **1**: 399–409.
26. Muñoz V, Serrano L. Elucidating the folding problem of helical peptide using empirical parameters, II. Helix macrodipole effects and the rational modification of helical content of natural peptides. *J. Mol. Biol.* 1994; **245**: 275–296.
27. Muñoz V, Serrano L. Elucidating the folding problem of helical peptide using empirical parameters, III. Temperature and pH dependence. *J. Mol. Biol.* 1994; **245**: 297–308.
28. Valente AP, Miyamoto CA, Almeida FCL. Implications of protein conformational diversity for binding and development of new biological active compounds. *Curr. Med. Chem.* 2006; **13**: 3697–3703.
29. Roche S, Rey FA, Gaudin Y, Bressanelli S. Structure of the prefusion form of the vesicular stomatitis virus glycoprotein G. *Science* 2007; **315**: 843–848.




DOI: 10.1002/psc